HiSST: 3rd International Conference on High-Speed Vehicle Science Technology

14 -19 April 2024, Busan, Korea

The Red Kite Sounding Rocket Motor Qualification Milestones and Application Spectrum

F. Scheuerpflug[1], T. Röhr[1], T. Huber[1], M. Reinold[1],
D. Hargarten[1], L. Kobow[1], R. Kirchhartz[1]
And
M. Kuhn[2], A. Weigand[2], M. Berndl[2], J. Werneth[2]

Abstract

The Red Kite© is a commercially available, serially produced solid propellant sounding rocket motor in the class of one ton of net explosive mass. It was developed in response to a sustained demand from the scientific community for high performance sounding rocket vehicles. The Red Kite is primarily designed to be employed as a powerful booster for military surplus and commercial second stages, but can also be used as a sustainer when boosted by either an even larger motor or by another Red Kite. Typical payloads will range between 200 to 600 kg. When used in a mission design tailored to microgravity research, typical apogees range between 250 to 300 km, while the needs of the hypersonic community can be met by a suppressed trajectory design, typically providing horizontal flight at Mach numbers between 6 to 9 in the altitude band 30 to 60 km. Following a Phase A definition study in 2017, the German Aerospace Center DLR contracted Bayern-Chemie GmbH in 2020 for the development and manufacturing of the Red Kite motor, initially providing 30 serial units. Subsequent to preliminary design and materials selection phase, ground testing of mechanical, pyrotechnical and electrical subsystems was conducted. Finally, two full scale qualification motors were successfully test-fired in August 2023 at ESRANGE Space Center, with the test models tempered to the upper and lower limits of the operational temperature envelope after having completed a rigorous protocol of thermal cycling and mechanical vibration representative of loads to be expected during handling, transport and flight. Following the successful qualification, serial production was initiated and serial motor number one released for a maiden flight from Andøya Space Center in November 2023, proving the design in flight successfully. The paper gives a summary of the motor performance, aspects of the system design, the qualification program and its application spectrum in active and future sounding rocket vehicles.

Keywords: *SOUNDING ROCKET, ROCKET MOTOR, RED KITE, MORABA, HYPERSONIC*

Nomenclature

ATHEAt	Advanced Technologies for High Energetic Atmospheric Flight of Launcher Stages – a DLR rocket borne research program	ITAR	International Traffic in Arms Regulations
BB	Black Brant Mk4 (Rocket Motor)	MAPHEUS	Materialphysikalische Experimente Unter Schwerelosigkeit – a DLR rocket borne research program
DLR	German Aerospace Center	MEOP	Maximum Expected Operating Pressure

[1] *DLR Mobile Rocket Base, 82234 Wessling*
[2] *Bayern-Chemie GmbH, 84544 Aschau am Inn*

EAR99	US Export Control Regulations	MORABA	Mobile Rocket Base
EFI	Exploding Foil Initiator	MTCR	Missile Technology Control Regime
ESRANGE	European Space and Sounding Rocket Range	NATO	North Atlantic Treaty Organization
GNSS	Global Navigation Satellite System	PATRIOT	Surface to Air Missile System
HAWK	Surface to Air Missile System	RK	Red Kite (Rocket Motor)
HTS	Horizontal Test Stand	STANAG	NATO Standardization Agreement
IM	Improved Malemute (Rocket Motor)	SID	Safe and Ignition Device
IO	Improved Orion (Rocket Motor)	VSB-30	Brazilian Sounding Rocket

1. Introduction

Pursuing our mission statement to support rocket borne science experiments from all over the world, MORABA has launched some 100 rockets in the past ten years and more than 500 since its foundation in 1965. Initially focused on experiments in atmospheric physics and astronomy, the spectrum has widened to microgravity research in material physics, biology, and space technology. From 2005 onwards, a sustained and increasing demand to support research regarding re-entry and highspeed atmospheric flight has emerged. We have responded to this demand by adapting our vehicle hardware and design capabilities accordingly, with major efforts to cope with the elevated thermal and mechanical loads inherent to hypersonic supressed trajectories. The addition of this growing research field however led to an increase in launch frequency and soon a critical bottleneck in the provision of suitable rocket motors.

It was under these circumstances that a Phase A study was conducted together with the German solid propulsion systems manufacturer Bayern-Chemie GmbH in 2017 [20] to define the characteristics of a motor that would fill this gap. The result was a 900 kg net explosive mass solid propellant motor with a total action time below 15 s that could be employed as a powerful booster for available commercial and military surplus upper stages as well as in tandem configuration of two units. DLR management approved of the concept and work plan and Bayern-Chemie GmbH was contracted in the beginning of 2020 for the joint development and subsequent production of 30 serial units. The project and the motor stage were dubbed after the European bird of prey "Red Kite". The present paper is a follow-up of an according publication [19] which now also includes results of the final development milestones such as two full scale static firings, one single stage test flight and an updated performance estimation and application spectrum of vehicles based on the Red Kite.

2. Motor Description

2.1. Major Design Requirements

The motor design was driven by a set of five requirements:

I. Performance of >400 kg to 250 km apogee on an up-and-over trajectory when used in two stage configuration or with a military surplus second stage.

II. Compatibility with existing launcher and vehicle hardware (in particular interstage, motor adapter and fin assembly).

III. Compatibility with ESRANGE Space Center's impact dispersion requirements [6] (for both single and multi-stage application).

IV. Limit export complexity for operations in and outside the European Union by avoiding critical material where possible.

V. Design with focus on ease of handling, cost efficiency and development risk.

Compatibility with existing hardware and launchers (II) facilitates a quick adoption of the new motor in our sounding rocket portfolio and reduces cost and complexity of manufacturing lines by allowing to produce fewer parts in larger quantities. The performance requirement (I) determined the motor propellant mass while compliance with acceptable dispersion limits at ESRANGE Space Center (III) drove the initial thrust. Since the payload capacity of a multi-stage vehicle is comparably insensitive to structural mass of the booster (depending on configuration, a saving of around 50 kg booster mass only translates into roughly a 9 kg increased payload capacity), extreme lightweight design, elaborate manufacturing techniques and materials were excluded from the development (V) to ensure short development timeline and a competitive pricing of the motor.

2.2. Main Characteristics

The Red Kite features a fin over cylinder grain design, an electronic Safe and Ignition Device (SID) which initiates a pyrogenic igniter and a submerged expansion nozzle design.

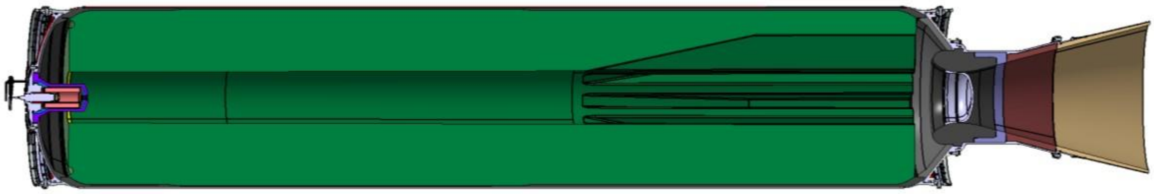

Figure 1: Red Kite Half Cut illustrating Finocyl Grain , Submerged Nozzle Design and Igniter Assembly [4]

Table 1: Red Kite Main Characteristics (nominal at +10°C)

Parameter	Units	Value
Gross Mass	[kg]	~1170
Propellant Mass	[kg]	~910
Structural Coefficient	[%]	~23
Main Diameter	[mm] [inch]	559 22
Length (Front Flange to Nozzle Exit)	[m]	3.440
Specific Impulse	[m/s]	~2510
Total Impulse (Vacuum)	[MNs]	2.3
Burn Duration (T = 10°C)	[s]	~13
Maximum Thrust (Vacuum)	[kN]	~240

Figure 2: Two Red Kites during preparations for the qualification firings

Motor chamber, as well as front and aft domes and parts of the nozzle assembly are manufactured from high-strength steel. Compared to fibre reinforced materials, this choice yields excellent handling robustness. It also eliminates or at least ameliorates the need for thermal barrier coating of the motor case to prevent structural impairment by excessive kinetic heating when the motor is employed in hypersonic mission designs.

The fin section is placed in the aft section of the propellant grain for optimal weight balance and minimal internal flow Mach number, thereby adding to vehicle static stability and aiding internal ballistics.

The Safe and Ignition Device is a commercially available, non-interrupted, electronic device based on capacitor discharge and exploding foil initiator technology that is commonly used in military systems, but first time adopted in a sounding rocket motor.

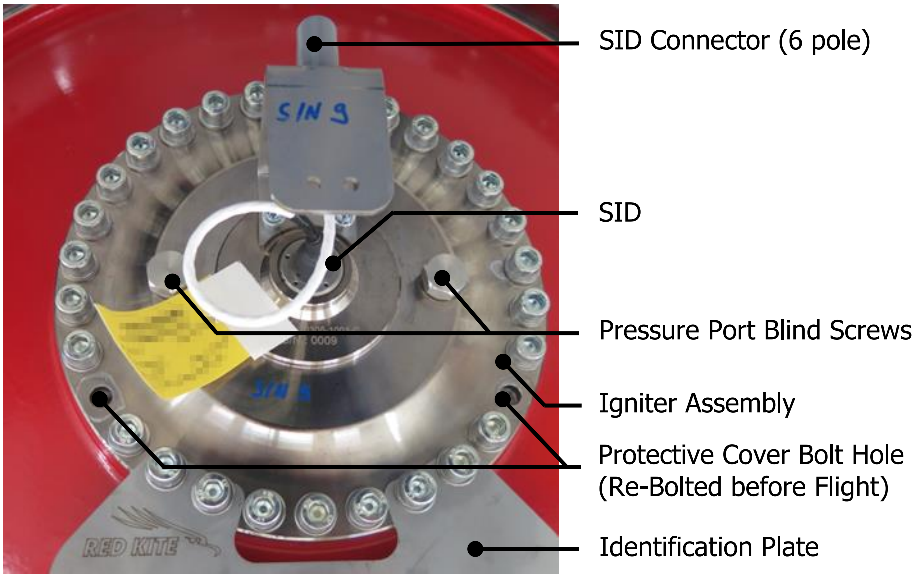

Figure 3: Red Kite Igniter After Removal of Protective Transport Cover

The nozzle assembly is realized as a submerged design to comply with a maximum length constraint imposed by a hardware compatibility requirement and also provides advantages in the thermal design and erosion of the aft dome insulation [14]. Graphite is used in the throat insert and the following two sections to warrant resistance to thermal shock and minimize erosion, while carbon fibre reinforced phenolic is used in the nozzle extension to minimize weight.

2.3. Interfaces

Mechanical front and aft interfaces are realized akin to the lap joint design used in the design of the VSB-30 [16]. By doing so, interfacing flight hardware such as boost adapters, motor adapters or tail cans can be produced in larger numbers lowering cost and simplifying procurement.

Figure 4: Front Mechanical Interface Joint and Igniter Assembly with SID and two pressure sensors installed

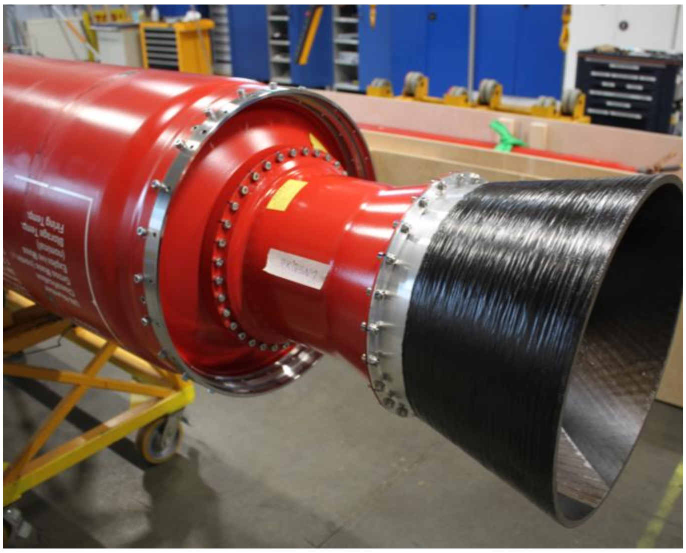

Figure 5: Aft Mechanical Interface Joint and Nozzle Assembly

The lap joint is a simple design that minimizes manufacturing and assembly cost at the expense of joint stiffness. This is an acceptable drawback due to the large joint diameter (545mm) and therefore inherent stiffness. It is also somewhat relieved in flight, when thrust and aerodynamic drag exert large compression forces on the joint, causing loads to be transmitted over an arrest rim of the interfaces rather than the radial joint bolts. The motor interfaces carry a thread pattern of M8x1 over a 15° pitch circle plus some additional M8x1/M10x1 threads at the motor datum axis (0° circumference) for launch lug fixation.

To monitor motor chamber pressure during burn, the igniter assembly features two M10x1 threaded holes as potential interfaces to a pressure sensor.

The electrical interface to the SID is realized via a six pole Glenair "Mighty Mouse" male connector of type 805-004-07M8-6PA [4], see also Figure 10.

2.4. Thrust Performance

The Red Kite was designed as a dual thrust burner, see Figure 6. High initial thrust warrants high acceleration at launch, which effectively reduces the trajectory dispersion of unguided sounding rockets caused by prevalent side winds. Vehicle acceleration rises as propellant is consumed and the accelerated mass reduced. To limit g-loads to a level compatible with delicate payloads (e.g biological probes) the thrust design features a subsequent low thrust phase until a steep tail-off ends the burn. For example, a Red Kite – Red Kite configuration carrying a 400 kg payload delivers a launch acceleration above 5 g while the maximum acceleration level remains below 17 g, see Figure 8.

Figure 6 also illustrates the temperature dependency of the thrust profile. To enable launches from arctic as well as tropical launch ranges without requiring thermal conditioning equipment, the motor was qualified for firing within a window of -20°C to +50°C. The propellant burn rate is notably higher for a warmer propellant grain causing a relevant variance in thrust level, but also in burn time.

- At -20°C soak temperature, a maximum vacuum thrust level of 225 kN is generated with burnout at 13.5 s.
- At +50°C soak temperature, a maximum vacuum thrust level of 255 kN is generated with burnout at 12.0 s

While the total impulse delivered to the vehicle (and hence, trajectory performance) is not affected significantly by the firing temperature, the variation in burn time may be relevant in the design of multistage vehicles. Given the large heat capacity of the motor and the propellant, it does however take many hours to even days of exposure for the propellant grain to fully reach thermal equilibrium with the environment.

Figure 7 depicts how the center of gravity, measured from the shoulder of the forward interface flange, moves during the burn. Due to its large burning surface, the aft fin section of the propellant grain is entirely consumed during the first seconds of the burn and the center of gravity moves forward accordingly. This aids the static stability of unguided sounding rocket vehicles during their early flight phase, when static stability margins are typically low.

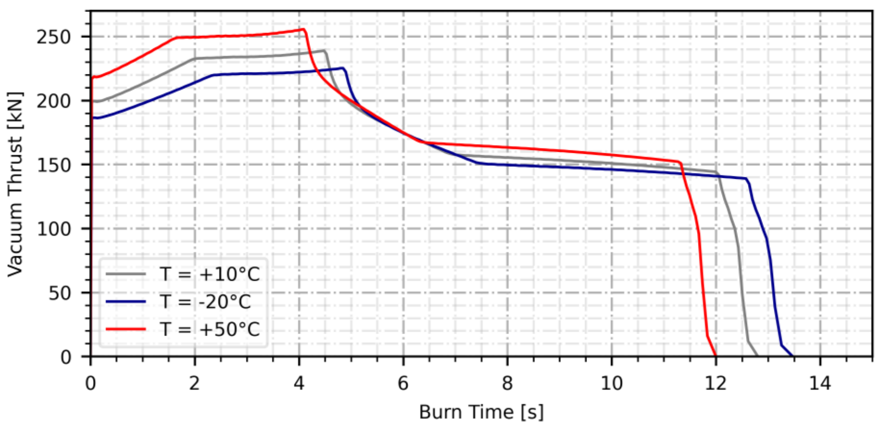

Figure 6: Red Kite Thrust Performance within Operational Temperature Range (-20°C to +50°C)

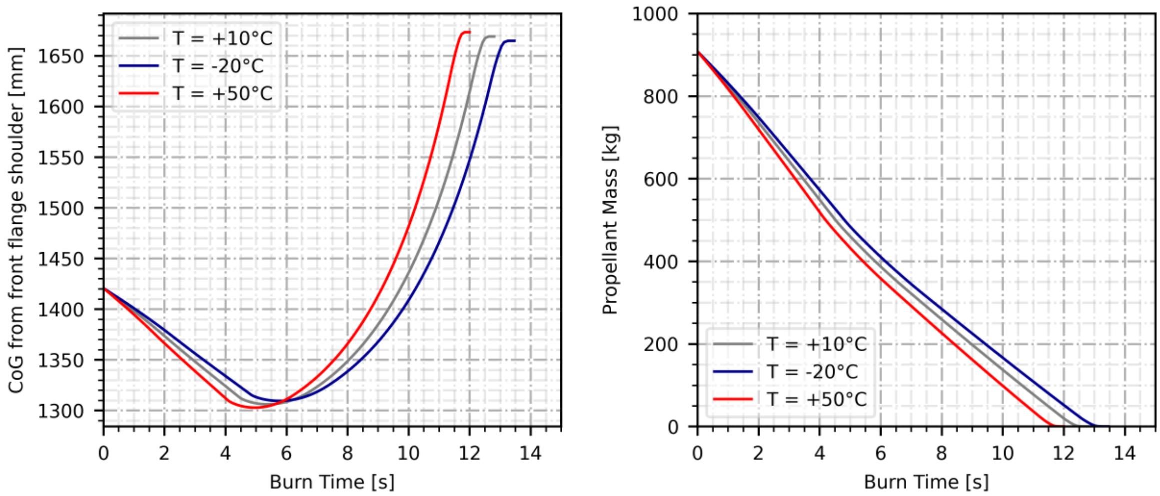

Figure 7: Red Kite Propellant Centre of Gravity and Consumption within Operational Temperature Range (-20°C to +50°C)

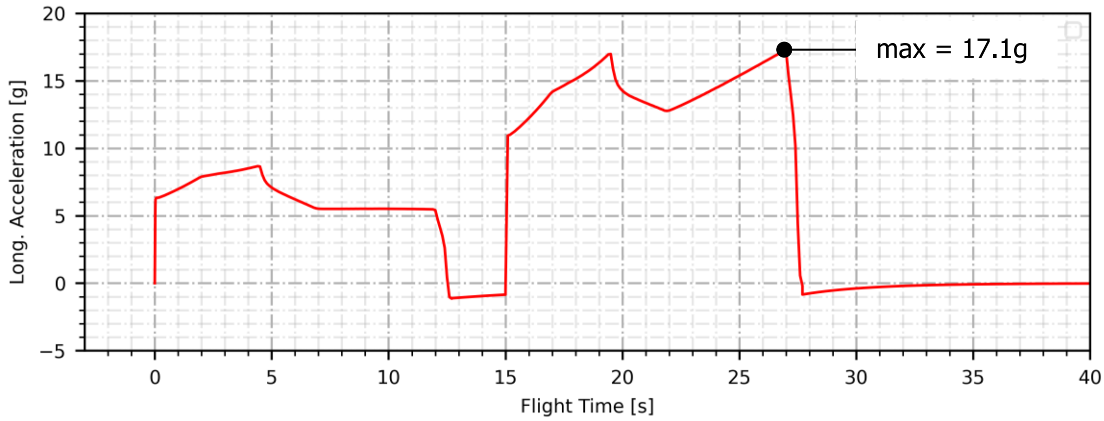

Figure 8: Longitudinal Acceleration Profile on a Red Kite - Red Kite vehicle for a typical up-and-over trajectory carrying a 400kg payload

2.5. SID & Safety

For the first time in a sounding rocket motor, the Red Kite pyrotechnic chain is initiated by an Exploding Foil Initiator (EFI) device. As opposed to the commonly used bridge wire initiators, an EFI offers intrinsic safety due to its insensitivity to stray electric currents, electrostatic discharge and electromagnetic radiation. The two-fault tolerance of an ignition device demanded by rocket launch ranges [6, 7] and design standards [5, 12] is met by the selected electronic Safe and Ignition Device. The unit is commercial of the shelf and primarily used in military application. Compared to commonly used manually or electrically driven, interrupted Safe Arm Devices, the SID offers reduced complexity, cost and mass budget.

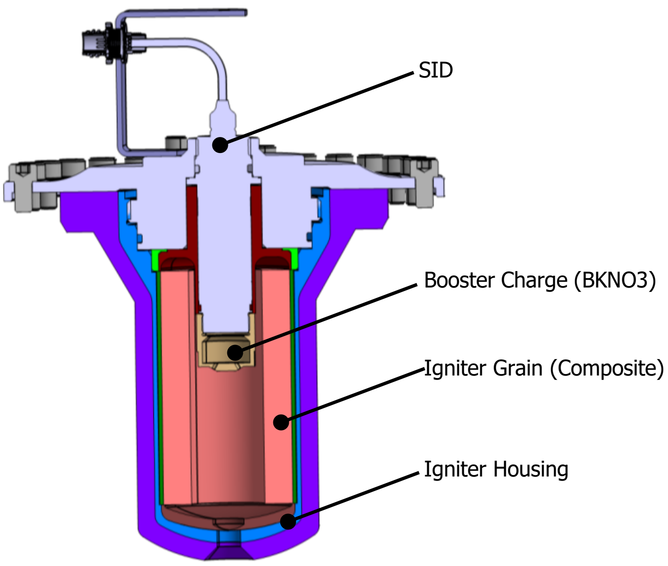

Figure 9: Igniter Assembly cross section

Figure 10: SID with connector

The electrical interface is composed of six pins. Two are shorted inside the Glenair connector and used to verify proper connection with the Arming Console. Another two pins are used to provide an 28V DC signal that steps the SID into an armed state and enables acceptance of the 28V DC firing signal on the two remaining pins. A dedicated 19” Arming Console was built to provide the monitoring, arming and firing functionality, see Figure 11.

Figure 11: Red Kite Arming Console

2.6. Shipping and Storage

To allow shipment of the motor to launch ranges around the globe, compatibility with air, sea and land freight requirements was required. The motor is shipped fully assembled with SID, igniter and nozzle assembly, in a wooden box, see images and dimensions in the below pictures and table.

Figure 12: Red Kite Motors in their reusable Transport Containers

Table 2: Main Characteristics of the Red Kite in its Transport Container [4]

Parameter	Units	Value
Gross Mass ca.	[kg]	1368
Net Explosive Mass	[kg]	915
Empty Mass ca.	[kg]	186
Length	[m]	3.7
Width	[m]	0.75
Height	[m]	0.86
Hazardous Goods Class	[ ]	1.2C
UN-No.	[ ]	0281

Shipping the motor in thrust-capable configuration also necessitates only a minimum amount of effort by vehicle assembly teams to prepare the motor for flight. Removal of protective covers over nozzle and igniter assembly, tightening of the two pressure ports and visual inspection of motor case, nozzle and forward dome are all that is required before adjacent hardware may be installed. In contrast to other rocket motors on the market, which are delivered only partially assembled, and in particular to military surplus rocket motors that oftentimes require extensive internal inspection, repair and leak checking, employment of the Red Kite saves a significant amount of time on the launch range and reduces related project risks.

The Red Kite is neither subject to ITAR nor EAR99 regulations, however German-national, EU Dual-Use and MTCR export control regulations do apply for any solid rocket motor of its class.

The Red Kite is certified for a shelf life of eleven years from production date when stored under controlled temperature (15° to 25° C) and humidity (arid) conditions.

3. Major Qualification Milestones

3.1. Component Testing & Qualification

The qualification program foresaw isolated tests of critical components and subassemblies to select and characterize materials and prove compliance with performance requirements prior to manufacturing of two full scale qualification motors. Table 3 summarizes the scope of the most prominent tests.

Table 3: Test and qualification of selected subcomponents

Component	Test	Objective	Quarter
Propellant	Accelerated aging at elevated temperature	Prove acceptable mechanical & chemical properties throughout motor shelf life (10+1 years)	Q2 2021
Nozzle	Several Burns of subscale items	Characterize materials	Q1 2021
Motor Case	Burst Test	Validate margin of safety	Q4 2021
Igniter	Several Test Firings	Validate pyrotechnic ignition chain and Igniter hot gas output	Q2 2022
Igniter	Qualification Firings of two units each tempered to +50°C and -20°C after environmental testing	Validate proper hot gas output after environmental testing comprising thermal shock, diurnal cycling as well as mechanical shock and vibrations during road and air transport (see section 3.2)	Q4 2022
Nozzle Seal	Pressure Test of Nozzle Seal	Validate burst pressure within interval to safely warrant main propellant grain ignition	Q3 2022
Nozzle Assembly	Full Scale Overpressure Test Firings	Validate nozzle assembly strength and thermal shock resilience in two firings that featured 2 s burns at pressures beyond Red Kite maximum expected operating pressure	Q4 2022

Figure 13: Subscale test firing to characterize nozzle material candidate

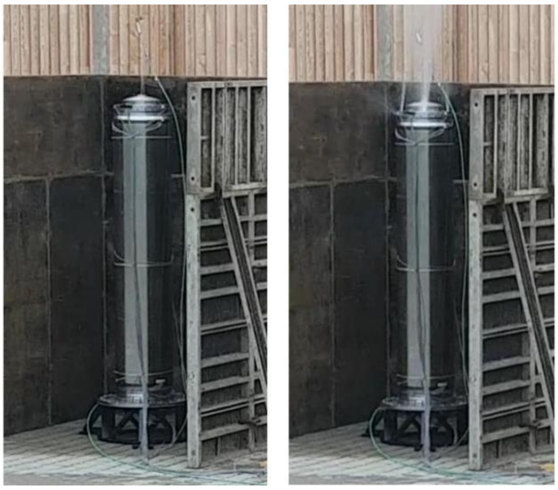

Figure 14: Motor case hydraulic burst test to validate margin of safety against Red Kite MEOP

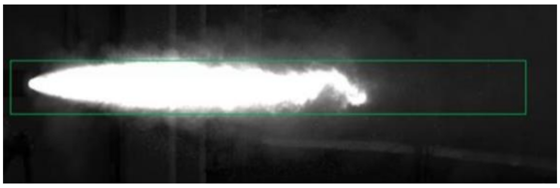

Figure 15: Igniter freestream firing (green area represents propellant bore diameter)

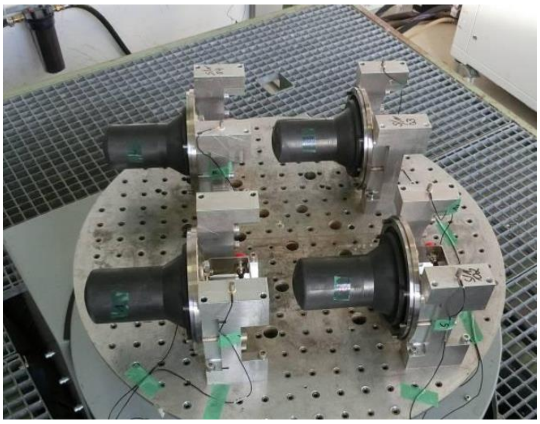

Figure 16: Vibration test of four igniter qualification units

Figure 17: Burst test of nozzle seal

Figure 18: 2s overpressure test of full scale nozzle assembly to validate mechanical strength and thermal shock resilience

3.2. Environmental Testing and Qualification Firings

Two static firings of full-scale qualification motors were conducted in August 2023 at the HTS-1 (Horizontal Test Stand) facility of ESRANGE Space Center. Both motors had previously been submitted to an extensive environmental testing program comprising thermal cycling and vibration loads that may be inflicted during storage, air and road transport as well as ground handling and flight. In particular, both motors were, according to requirements, consecutively subjected to:

- Thermal diurnal cycling (10 days) in hot and cold conditions (according to [1, 3]), simulating dwell time in arctic and tropic conditions during transport and storage.
- Shock and vibration equivalent to 7000 km of ground wheeled common carrier transport (according to [2]) including loading operations.
- Shock and vibration equivalent to 20h flight each, assuming two different fixed wing propeller aircraft (C-130 in 4 and 6 blade configuration, according to [2]).
- Operational vibration load of 12 s in three axes, reflecting the load imposed on the motor by a booster motor when used as upper stage (adopted from [15]). Power constraint of available

vibration tables limited the levels tested to 5.4 grms from 20 to 600 Hz, thereby undertesting the specified 12.7 grms from 20 to 2000 Hz.

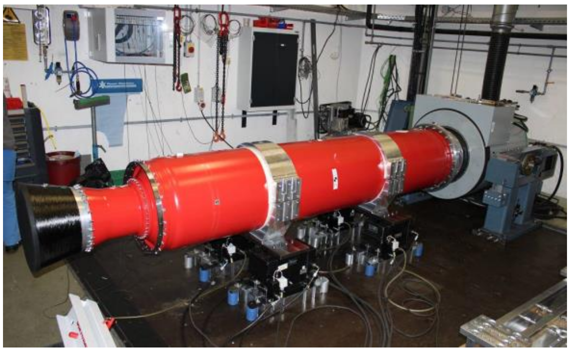

Figure 19: Red Kite qualification motor during longitudinal vibration test

Figure 20: Qualification motor in climate chamber for thermal cycling

The motors passed prior and subsequent visual and x-ray inspection showing no signs of wear, cracks or delamination inside the propellant block and motor chamber and were released for the qualification firings. In order to test the operational firing envelope of the motor, specified to -20°C to +50°C, the two qualification motors were accordingly climatized for a duration of three days, while test bench and instrumentation was prepared.

Figure 21: Red Kite Qualification Motor #1 at -20°C being moved to HTS-1

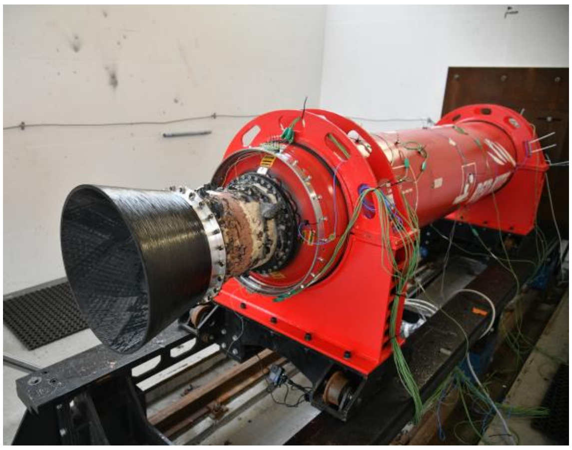

Figure 22: Motor instrumented and fixated on the test bench of HTS-1 (post-firing)

Test instrumentation comprised equipment to validate motor performance and engineering safety margins:

- A PT700 load cell sampled at 20 kHz.
- Pressure sensors in the two ports of the motor sampled at 5 and 20 kHz.
- Vibration sensors mounted on the front dome, central motor case and aft dome sampled at 50 kHz. Another one was mounted on the cylindrical load transmission adapter skin and sampled at 5 kHz.
- Strain gauges distributed over the motor and nozzle assembly skin.
- Temperature couples distributed over the motor and nozzle assembly skin.
- Diverse camera and spectroscopy equipment (infrared, ultraviolet, visual) sampled at varying rates monitoring motor, nozzle and exhaust plume.

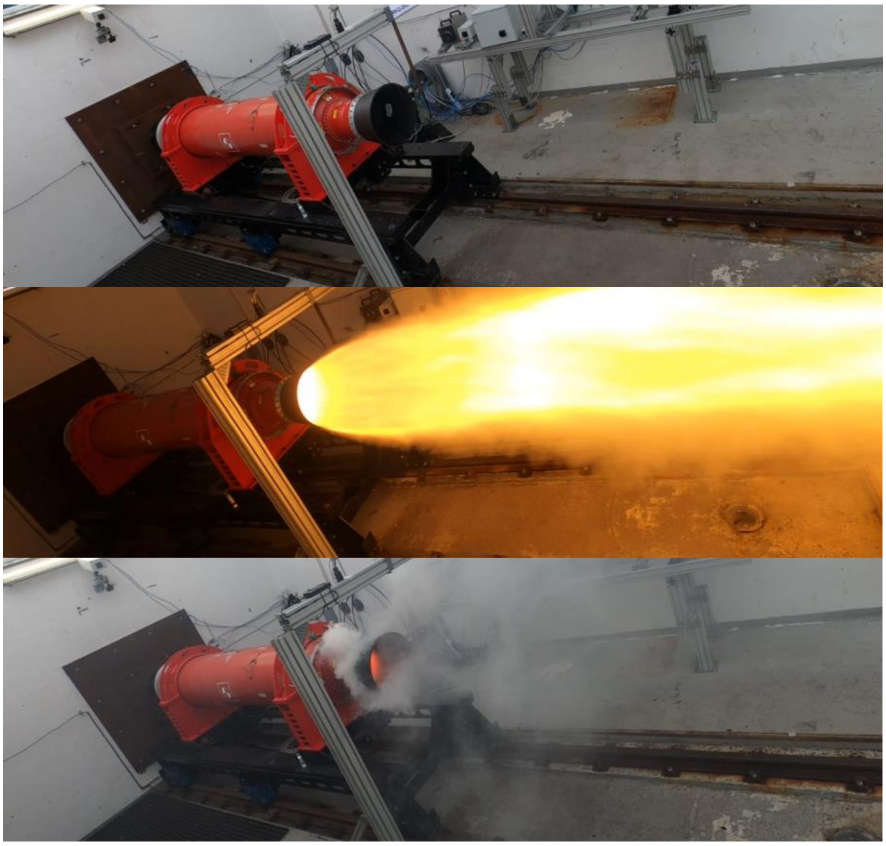

Figure 23: Photo sequence of the +50°C firing

Data collected during these firings and also post-test visual and destructive investigation of the motor chamber, igniter assembly and nozzle validated motor performance and engineering safety margins in full compliance with requirements. In particular:

- Thrust and pressure data obtained were in good agreement with predictions and used for refinement of the ballistic model which forms the basis of performance predictions of the serial units (see Figure 6).
- No significant signs of combustion instabilities were observed.
- Safety margins, especially with regards to thermal insulation were found to be generous, opening up possibilities for improved performance by minor adjustment of the design in the future.
- Steady and steep tail-off was confirmed.
- Motor case, front and aft dome temperatures increased only by single degrees centigrade during the burn phase, while some exterior parts of the nozzle heated up to about 100° C during the burn phase.
- Vibration magnitudes about 2-3 grms were recorded on the exterior skin of the cylindrical load transmission adapter in all three axes, while the motor case vibrated at about 7 grms in all three axes at its central location.

Subsequent to the firings, the serial production of the Red Kite was initiated.

3.3. Qualification Flight

The first serial motor was submitted to a single stage test flight from Andøya Space Center in November 2023 [18]. In addition to a set of basic diagnostic equipment consisting of GNSS, 3-axis gyroscope, 3-axis accelerometer, motor chamber pressure and a vibration sensor, the flight carried an onboard camera and scientific payload that investigated the aerodynamics of a rotationally symmetric scramjet inlet and internal flow path [17]. The flight was also skin tracked by the RIR-774C radar to obtain trajectory information independent of onboard systems.

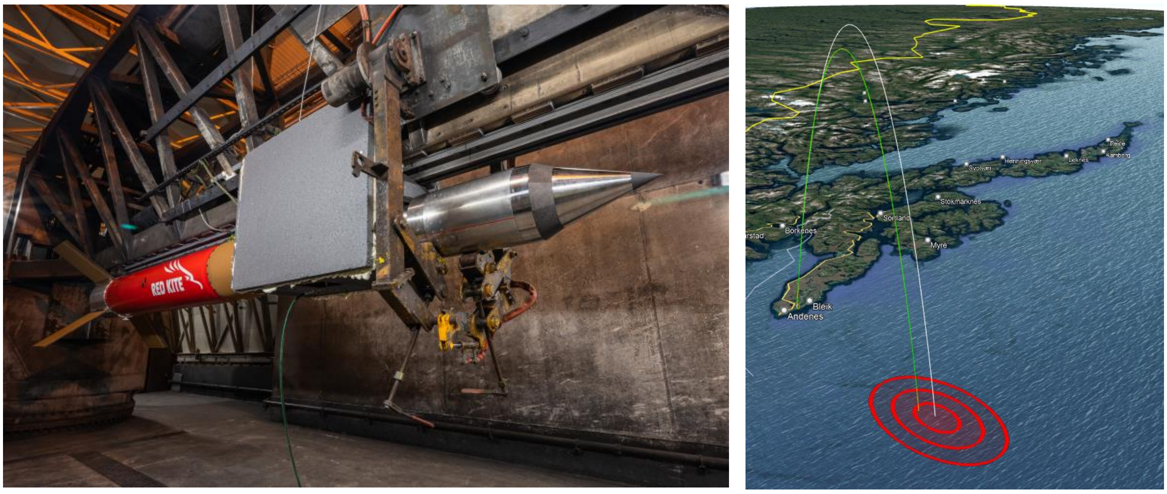

Figure 24: Red Kite test flight vehicle on the launcher
right: perspective on nominal (white) and actual (green) trajectory with 1, 2 and 3-sigma impact dispersion ellipses

Figure 25: Lift-Off from U3 launcher at Andøya Space Center

Vehicle and payload data (including motor pressure, 3-axis gyroscope, 3-axis accelerometer and GNSS) were transmitted to ground via S-Band downlink as the flight was planned to impact in the open sea without recovery or retrieval. Transmission was received continuously from launch to 235 m before impact. Analysis of flight data proved motor performance close to prediction and vehicle dynamics nominal. In particular, the attitude behavior of the spin-stabilized rocket did not display evidence of anomalies such as thrust misalignment or dynamic instabilities. Thrust misalignment can originate from geometrical asymmetry of the motor case, nozzle or propellant cast, distortion upon pressurization, asymmetric nozzle erosion or transient gas flow phenomena [13]. These factors had been given consideration in the motor design and propellant casting to minimize thrust misalignment but neither the component tests nor the qualification firings could be properly instrumented to obtain a reliable quantitative measure. Final evaluation was therefore left to the test flight, where the free motion of the vehicle in its early flight phase provides an excellent opportunity to observe effects of thrust misalignment.

4. Application Spectrum

Based on the Red Kite, we intend to bring a whole family of vehicles into service. Figure 26 illustrates vehicles that are currently in their design phase or have already been launched.

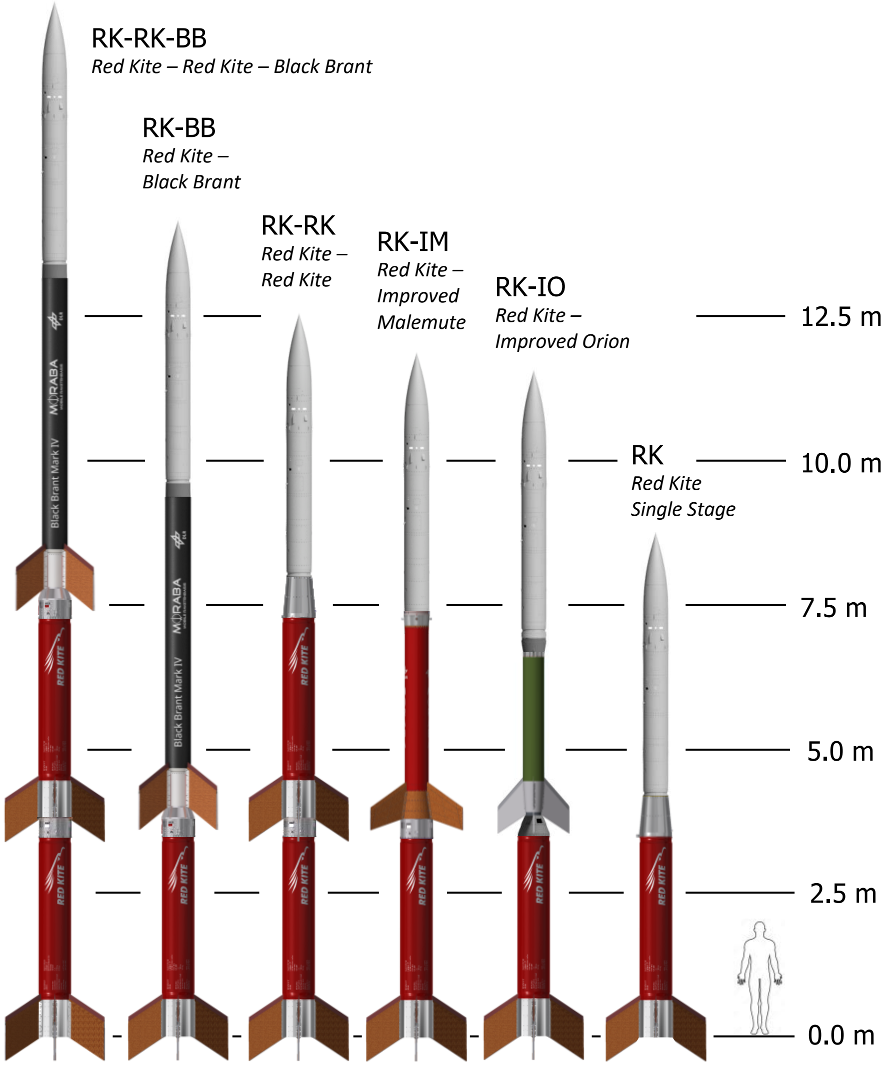

Figure 26: Family of vehicles based on the Red Kite motor

The performance characteristics of the Red Kite allow for staging with most of the other solid rocket motors operated by Mobile Rocket Base, enabling an almost continuous performance envelope, see Figure 32. The Red Kite will fly staged with another Red Kite, the military surplus motors Improved Orion (14” main diameter) and Improved Malemute (16” main diameter), and also with Magellan’s Black Brant Mk4 (17” main diameter). The Improved Orion and the Improved Malemute, which are demilitarized propulsion sections of the HAWK and PATRIOT missile defence systems, qualify as very cost efficient second stages. Both stages are relatively light weight which leads to high velocity gains during the Red Kite boosted flight phase and low impact point dispersion estimates, even when omitting spin induction motors, which reduces system complexity and launch cost. With one ton of composite propellant, the Black Brant Mk4 provides a total impulse of 2.5 MNs over a 27 s action time. A very powerful vehicle is formed when pairing it with a Red Kite as a first stage.

At the time of writing (March 2024), the RK-IM has recently been qualified successfully in the DLR MAPHEUS research program. The vehicle was launched from ESRANGE on February 27th 2024, and carried its 440 kg payload to an apogee of 265 km, providing more than six minutes of microgravity to the experiments on board. Motor pressure and vehicle attitude and acceleration were evaluated and confirmed nominal performance of the Red Kite.

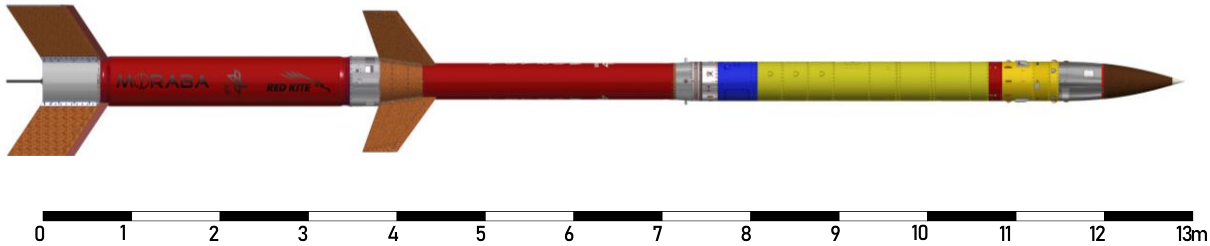

Figure 27: MAPHEUS-14, first flight of the Red Kite - Improved Malemute

Figure 28: MAPHEUS 14 inside the Skylark Launcher

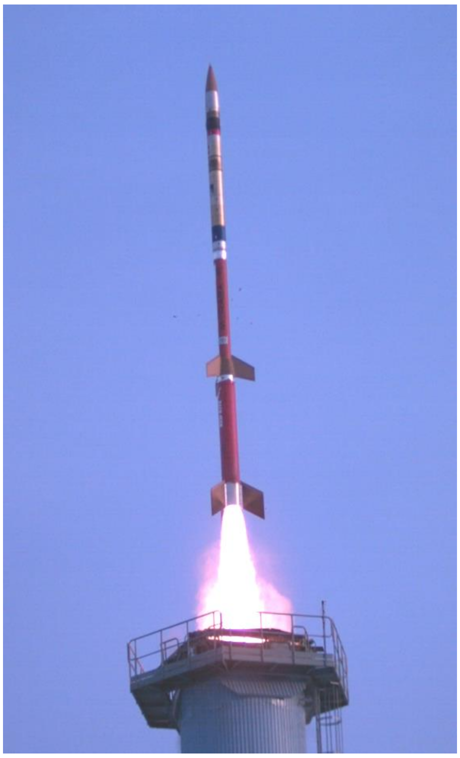

Figure 29: MAPHEUS 14 exiting the Skylark Launcher at ESRANGE Space Center at 08:27 local time

Next, we aim for a flight qualification of the Red Kite - Black Brant in 2025 in the frame of the ATHEAt hypersonics research project. Slated for launch in June 2025, the vehicle will perform a suppressed trajectory that provides atmospheric flight at Mach numbers above 8 for a duration of more than two minutes, see Figure 31. The flight will be conducted from Andøya Space Center in 2025. Apogee will be 55 km and impact ground range beyond 500 km. Payload mass is currently estimated to 195 kg.

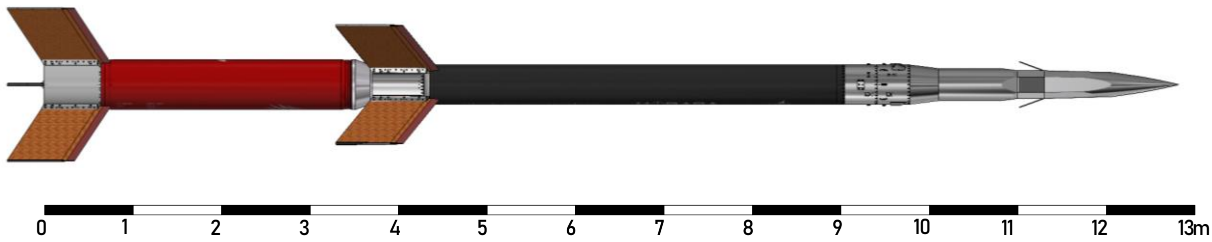

Figure 30: ATHEAT, first flight of the Red Kite - Black Brant Mk4

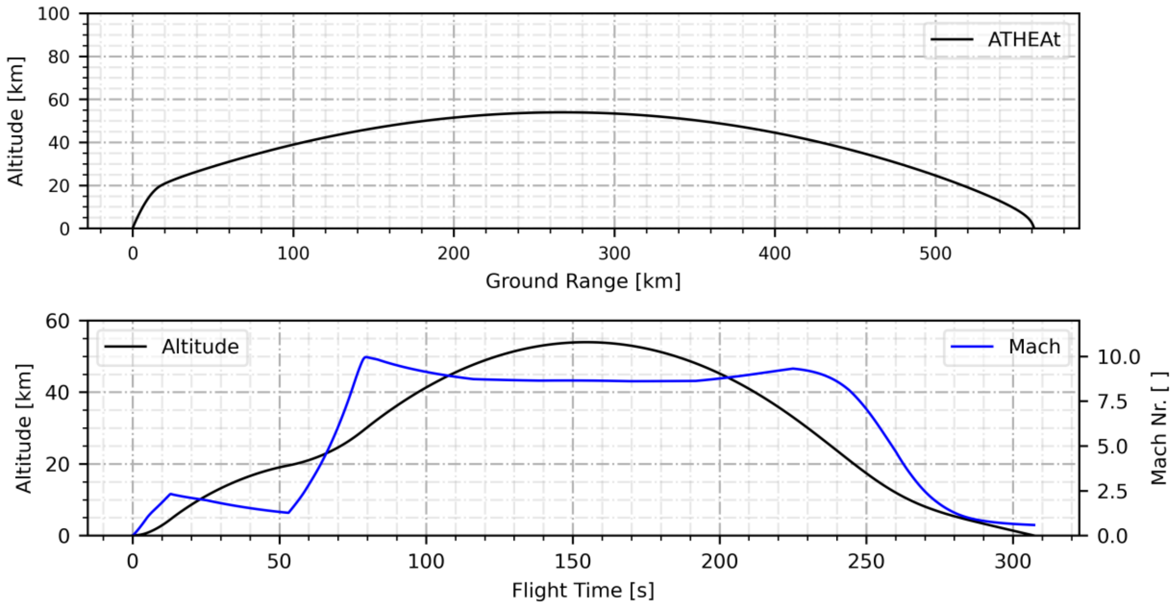

Figure 31: ATHEAt preliminary trajectory and flight Mach number

Beyond those programs, Red Kite based vehicles are currently in consideration for research programmes focussed on hypersonics, microgravity as well as atmospheric physics.

4.1. Apogee Performance of Vehicles based on Red Kite

To facilitate vehicle selection for projects requiring steep parabolic trajectories such as typically employed in microgravity research, a parametric analysis of apogee performance was conducted for all members of the Red Kite vehicle family, see Figure 32.

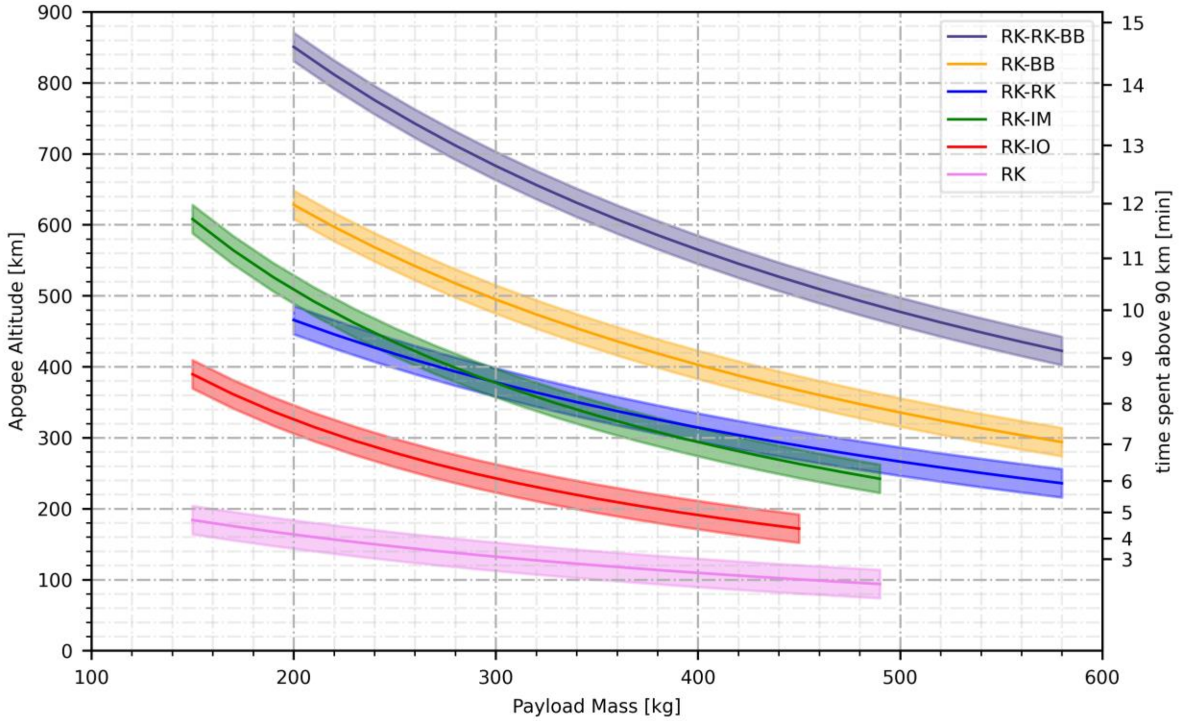

Figure 32: Apogee performance of the Red Kite family of vehicles. Right y-axis illustrates time spent above 90 km, i.e. possible research window under microgravity conditions

Payload mass given in the graph refers to all masses above the upper stage motor front flange. The estimates were derived assuming a typical 14″ diameter payload in case of the single stage Red Kite and typical 17″ diameter payloads for all other vehicles. Bandwidth given illustrates performance dependency on aerodynamic shape of the payload. The vehicle family fully covers a requirements envelope between 200-550 kg of payload mass and apogees beyond 800 km, equating to more than 14 min of possible micro-g experiment time.

Interestingly, the Red Kite – Improved Malemute outperforms the considerably heavier Red Kite – Red Kite for lighter payloads which is due to very low structural mass of this motor.

4.2. Hypersonics Testing

Trajectory designs in hypersonics vary greatly depending on payload requirements, payload maneuvering capability, launch range boundaries, telemetry coverage and recovery requirements. Many programs leverage the simplicity of a steep parabolic design (e.g. [8, 10]) which allows to use standard telemetry setups and recovery techniques at the expense of a short experiment duration (typically few seconds) and quickly varying flight condition during the near vertical atmospheric ascent and descent. Some fields of research however require extended duration (in the order of minutes) and/or accurate and quasi-constant flight conditions in hypersonic atmospheric flight. These conditions are accessed by suppressed trajectories that often do not leave the atmosphere at all, but insert payloads directly into their target altitude band (e.g. [9]). Implicitly, these trajectories lead to impact ground ranges of typically several hundreds of kilometers, posing challenges to telemetry setup, range safety and rendering payload recovery economically infeasible in many cases.

To obtain a baseline performance assessment of the Red Kite vehicle family in service of hypersonics testing, ballistic direct insertion trajectories where simulated assuming a 60 km target apogee, 300 kg payload mass and captive flight, i.e. payload remains attached to upper stage motor until impact, see Figure 33.

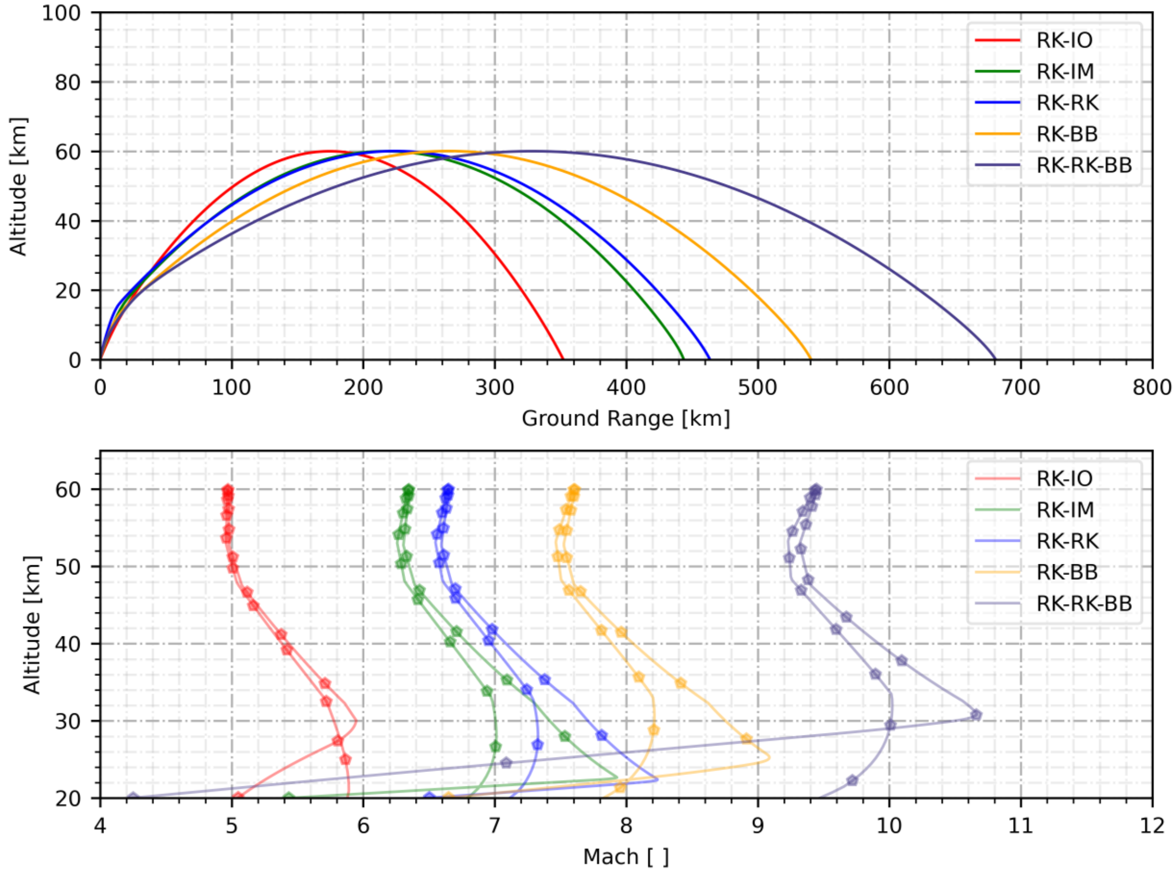

Figure 33: Hypersonics performance of vehicles based on Red Kite assuming 300 kg payload mass and ballistic trajectories with apogee 60 km. Markers indicate dwell time (10 s distance marker to marker)

The graph depicts trajectory shape as well as research conditions in the form of an Altitude vs. Mach number graph. To provide dwell time in the respective Mach regime, the curves are marked every 10 s of the flight.

Launch elevation and ignition time of upper stages were optimized for maximum Mach numbers during the experiment window. This results in an extended cost phase (few ten seconds) subsequent to booster burnout to effect gravity turn and achieve trajectory suppression. The curves are run through in counter-clockwise direction and distinctly show a part of the acceleration phase during the upper stage burn.

To provide an estimate of performance sensitivity towards payload mass, the same analyses were conducted assuming a payload mass of 200 kg, see Figure 34.

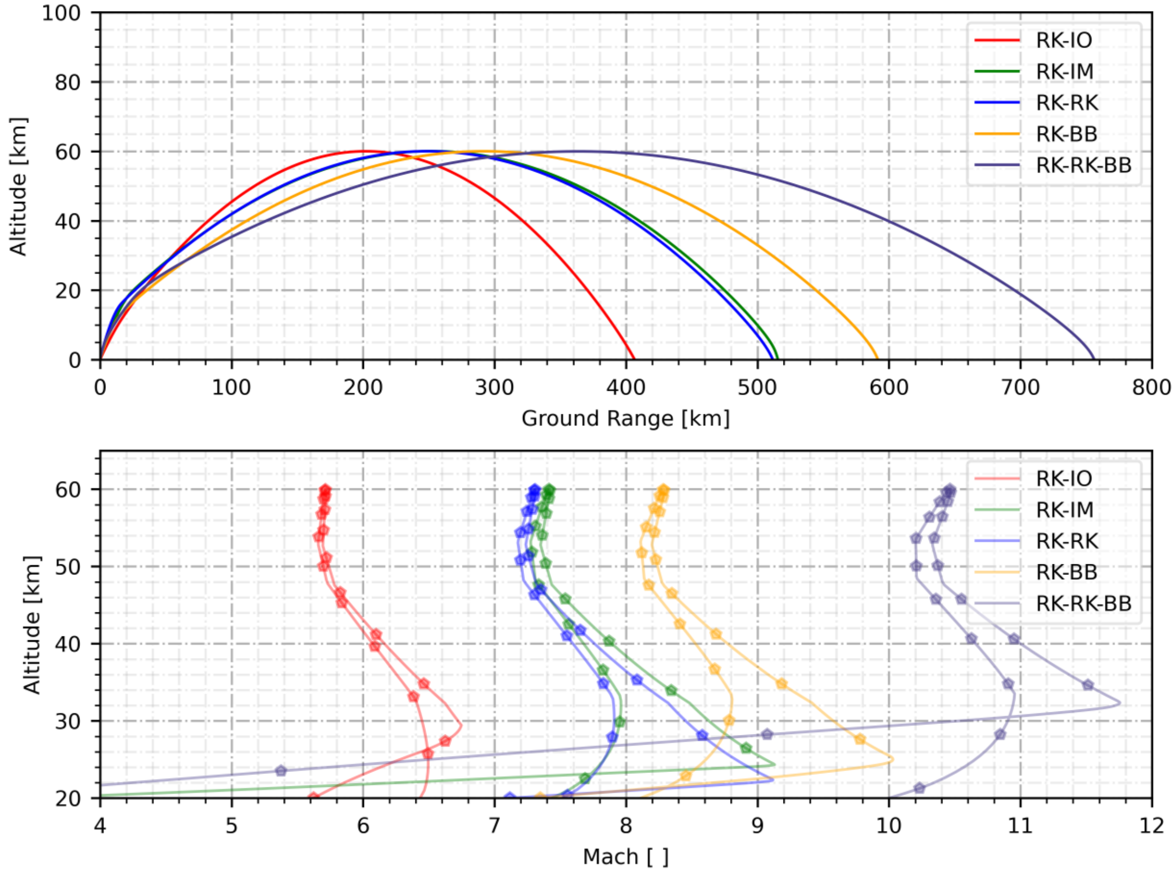

Figure 34: Hypersonics performance of vehicles based on Red Kite assuming 200 kg payload mass and ballistic trajectories with apogee 60 km. Markers indicate dwell time (10 s distance marker to marker)

Depending on the configuration, a reduction in payload mass of 100 kg raises the Mach level by a delta of 0.7-1.1.

5. Summary

The Red Kite solid rocket motor was designed as a powerful booster for a two-stage application with another Red Kite or a different motor of our portfolio. The development phase began in January 2020 and culminated in two successful static firing in August 2023. Serial production of 30 units was initiated and a single stage test flight conducted with nominal outcome in November 2023.

The Red Kite has since been used in two-stage configuration as a booster for an Improved Malemute upper stage, launched from ESRANGE in February 2024. The vehicle performed nominally and reached an apogee of 265 km. In the upcoming years, we foresee utilization of the motor on a regular basis and further expansion of the family of vehicles involving the Red Kite by pairing it with other rocket motors of our active portfolio. This encompasses all fields of our launch service, in particular microgravity research and hypersonics testing, but possibly also atmospheric physics.

Our Red Kite based portfolio offers a continuous performance envelope for payloads in the 150-600 kg class requiring insertion onto steep parabolas with apogees anywhere from 100-800 km. Using suppressed trajectory designs, payloads of several hundred kilograms mass can be launched into hypersonic, atmospheric flight up to and beyond Mach 10 for several minutes.

6. Acknowledments

The unique research opportunities accessed by the development and utilization of this new, commercial sounding rocket motor were recognized by DLR management and its then and now managing directors. Amongst others, the support and advocacy of Roland Pleger, Susann Groß, Hansjörg Dittus, Anke Pagels-Kerp and Felix Huber have made the project possible.

7. References

1. AECTP -300, Allied Environmental Conditions and Test Publications, NATO specific military environmental standards (climatic), Edition D Version 1, Nov. 2019
2. AECTP -400, Allied Environmental Conditions and Test Publications, NATO specific military environmental standards (mechanical), Edition 3, Jan. 2006
3. AECTP -230, Allied Environmental Conditions and Test Publications, NATO specific military environmental standards (climatic conditions), Edition 1, May 2009
4. Berndl et al., Red Kite Rocket Motor Handling and Safety Instructions, HHV-670-20300-0000-005, 02/2024, Bayern-Chemie GmbH, Aschau am Inn
5. ECSS-E-ST-33-11C Rev.1, 1 June 2017, Space Engineering, Explosive Subsystems and Devices
6. ESRANGE Safety Manual V9.0, June 2020
7. GSFC Wallops Flight Facility Range Safety Manual, GSFC-STD-8009
8. Gülhan, Thiele, Stamminger, Scheuerpflug et al., Main Achievements of the Rocket Technology Flight Experiment ROTEX-T, AIAA Test and Evaluation IV, 2017-2208
9. Gülhan, Hargarten, Zurkaulen, Klingenberg et al., Selected results of the hypersonic flight experiment STORT, Acta Astronautica, Volume 211, October 2023
10. Hörschgen-Eggers, Kirchhartz, Jung, Schoppmann, Ettl, Wittkamp, Boundary Layer Transit Flight Experiment: Mission Overview, Launch Vehicle and Payload Subsystems, Journal of Spacecraft and Rockets, Vol. 58, 2021
11. https://en.wikipedia.org/wiki/Slapper_detonator
12. Ignition Systems for Rockets and Guided Missile Motors – Safety Design Requirements, NATO STANAG 4368
13. Knauber et al., Thrust Misalignment of Fixed-Nozzle Solid Rocket Motors, Journal of Spacecraft and Rockets, Vol. 33, November-December 1996
14. Kuhn, Weigand, Berndl, Werneth, Scheuerpflug, Kirchhartz, Röhr – Red Kite Sounding Rocket Motor Qualification, Proceedings of the 26 ESA PAC Symposium 2024, Luzern
15. NSROC, NASA Sounding Rockets User Handbook, GSFC-810-HB-SRP, July 2015
16. Palmerio, da Silva, Turner, Jung, The Development of the VSB-30 Sounding Rocket Vehicle, 16th ESA Symposium on European Rocket and Balloon Programmes and Related Research, June 2003
17. Riehmer, Klingenberg, Röhr, Schnepf, Zuber, Gülhan, Design and Objectives of the Air-breathing Propulsion Experiment Technology Demonstrator (APEX-TD), 3rd International Conference on High-Speed Vehicle Science and Technology, 14.-19. April 2024, Busan
18. Röhr, Scheuerpflug, Riehmer, Zuber, Schnepf, Kirchhartz, Flight Qualification of the Red Kite Solid Rocket Motor, 3rd International Conference on High-Speed Vehicle Science and Technology, 14.-19. April 2024, Busan
19. Scheuerpflug, Weigand, Kuhn, Kirchhartz et al., Development and Projected Performance of the Red Kite Sounding Rocket Motor. 25th ESA Symposium on Sounding Rockets and Balloons, 1.-5. Mai 2022, Biarritz, ISBN 9789292213084, ISSN 0379-6566, https://elib.dlr.de/197879/
20. Scheuerpflug, Naumann, Weigand, Eggers, Ciezki, Study of a Rocket Motor Stage for Sounding Rockets, Oberpfaffenhofen, 2017
21. Stromsky, RAC – System Description, Version 1.0, 09/2023 Oberpfaffenhofen
22. Weigand, Ringeisen, Meyer, Naumann, Kirchhartz, Jung, Scheuerpflug, A Solid Propellant Rocket Motor for a Sounding Rocket, AIAA Propulsion and Energy Forum, 2020-3936, https://doi.org/10.2514/6.2020-3936